ORIGINAL ARTICLE

Decoding bilingualism from resting-state oscillatory network organization

Lucia Amoruso[1,2,3,#] 🔵 | **Adolfo M. García**[3,4,5,#] | **Sandra Pusil**[6] | **Polina Timofeeva**[1,7] | **Ileana Quiñones**[1,2] | **Manuel Carreiras**[1,2,7]

[1]Basque Center on Cognition, Brain and Language (BCBL), San Sebastian, Spain

[2]Ikerbasque, Basque Foundation for Science, Bilbao, Spain

[3]Cognitive Neuroscience Center (CNC), Universidad de San Andrés, Buenos Aires, Argentina

[4]Global Brain Health Institute, University of California San Francisco, San Francisco, California, USA

[5]Departamento de Lingüística y Literatura, Facultad de Humanidades, Universidad de Santiago de Chile, Santiago, Chile

[6]Center for Cognitive and Computational Neuroscience, Complutense University of Madrid, Madrid, Spain

[7]Universidad del País Vasco (UPV/EHU), San Sebastian, Spain

Correspondence
Lucia Amoruso, Basque Center on Cognition, Brain and Language (BCBL), 20009 San Sebastian, Spain. Email: l.amoruso@bcbl.eu

Abstract

Can lifelong bilingualism be robustly decoded from intrinsic brain connectivity? Can we determine, using a spectrally resolved approach, the oscillatory networks that better predict dual-language experience? We recorded resting-state magnetoencephalographic activity in highly proficient Spanish-Basque bilinguals and Spanish monolinguals, calculated functional connectivity at canonical frequency bands, and derived topological network properties using graph analysis. These features were fed into a machine learning classifier to establish how robustly they discriminated between the groups. The model showed excellent classification (AUC: 0.91 ± 0.12) between individuals in each group. The key drivers of classification were network strength in beta (15–30 Hz) and delta (2–4 Hz) rhythms. Further characterization of these networks revealed the involvement of temporal, cingulate, and fronto-parietal hubs likely underpinning the language and default-mode networks (DMNs). Complementary evidence from a correlation analysis showed that the top-ranked features that better discriminated individuals during rest also explained interindividual variability in second language (L2) proficiency within bilinguals, further supporting the robustness of the machine learning model in capturing trait-like markers of bilingualism. Overall, our results show that long-term experience with an L2 can be "brain-read" at a fine-grained level from resting-state oscillatory network organization, highlighting its pervasive impact, particularly within language and DMN networks.

[#]Indicates equal contribution.

- -

INTRODUCTION

Bilingualism has become a prevalent phenomenon in contemporary societies, with over half of the world's population engaging in active experiences with both a first (L1) and a second language (L2).[1] Recent evidence highlights the brain's remarkable ability to reorganize its structure and function in response to lifelong experiences, including sustained training in cognitive[2,3] and sensorimotor[4–6] skills. Considering the central role of language in daily communication, it is unsurprising that dual-language experience leads to neuroplastic adaptations in the human brain.[7,8]

Network-level measures, such as resting-state functional connectivity (rsFC), have proven effective in capturing such neuroplastic changes in bilingual individuals.[9–11] In essence, the acquisition of an L2 induces experience-dependent neural changes that alter communication patterns between brain regions, thereby influencing FC. These studies consistently show rsFC changes within language networks, including inferior frontal and temporal structures, and within cognitive control networks involving dorso-lateral prefrontal, parietal, supplementary motor, and anterior cingulate hubs, crucial for managing language interference.[12,13] Despite neuroimaging progress in unveiling "re-wiring" patterns in these critical networks, a fundamental question remains unanswered[14]: Can lifelong bilingualism be robustly decoded from rsFC? Moreover, based on novel spectrally resolved connectivity approaches: Can we determine which oscillatory networks better predict sustained dual-language experience?

Although functional magnetic resonance imaging (fMRI) has been extensively employed to study rsFC, it is blind to oscillatory information beyond the temporal range ($\sim$1 Hz) of the hemodynamic response it measures.[15] In contrast, high temporal resolution techniques like magneto/electroencephalography (M/EEG) are better suited for capturing the full spectral richness of brain recordings, thereby adding a new dimension to rsFC analysis.

Brain oscillations at different frequency bands are believed to serve distinct functions in network communication.[16] In the context of bilingualism, M/EEG research remains scarce, making it challenging to draw generalizable conclusions. However, available studies emphasize the prominent role of neural rhythms in explaining dependencies between variables describing network behavior and factors such as L2 age of acquisition (AoA) or L2 proficiency. Some studies have reported enhanced alpha (8–12 Hz) and beta (15–30 Hz) rsFC in bilinguals compared to monolinguals,[17,18] with alpha effects positively correlating with L2 AoA and proficiency measures. Moreover, evidence from bilinguals with varying L2 proficiency and AoA suggests that gamma (30–50 Hz) and beta rhythms can track individual differences in the extent of dual-language experience.[19] Longitudinal studies on L2 learning after immersive training[20–23] also reveal that beta rsFC along the right hemisphere correlates with post-training L2 learning outcomes. While evidence for the role of beta oscillations in bilingualism seems more consistent across studies, research on other brain rhythms like alpha and gamma calls for further exploration.

Beyond the oscillatory properties of brain networks, it is crucial to understand how these networks become organized to facilitate efficient information transfer. Graph theory provides a robust framework to study this topological organization,[24] offering measures to quantify properties at global (whole-network) and local (individual nodes or links) levels. Recent research indicates that global topological metrics within specific frequency bands effectively trace experience-dependent individual differences across various domains, including sensorimotor abilities and language learning outcomes. For instance, the characteristic path length, a global measure reflecting network integration, accurately differentiates expert dancers from novices within the sensorimotor mu range (8–13 Hz).[25] Similarly, the leaf fraction, another measure of whole-network integration, predicts improvements in L2 fluency following immersive training in the beta range.[26] These findings suggest that global topological properties can serve as trait-like fingerprints for identifying individuals with varying neurocognitive profiles.

Here, we aimed to examine the impact of lifelong bilingualism on intrinsic oscillatory network configuration and its potential for classifying individuals based on dual-language experience. We computed graph-theory measures from spectrally resolved magnetoencephalographic (MEG) rsFC data and employed machine learning techniques to assess their robustness in differentiating between bilinguals and monolinguals. Additionally, we explored whether these measures could predict individual variations in L2 proficiency. We hypothesized that global topological metrics, likely in the beta band, would distinguish individuals based on their bilingual experience, particularly within networks involved in language processing and/or cognitive control. Furthermore, we anticipated that these features would correlate with L2 proficiency. With this approach, we aimed to forge a more fine-grained view of how bilingualism shapes intrinsic brain organization.

MATERIALS AND METHODS

Participants

The study involved 44 participants, namely: 22 Spanish-Basque highly proficient bilinguals and 22 Spanish monolinguals. However, four participants were removed from all analyses as their MEG recordings presented substantial muscular and eye-related artifacts. Thus, the final sample comprised 20 bilinguals (age range: 19–45 years) and 20 monolinguals (age range: 21–45 years). All participants were

TABLE 1 Descriptive and inferential statistics for each variable.

		Bilinguals (*n* = 20)	Monolinguals (*n* = 20)	*p*-value
Demographics	Sex (M:F)	7:13	9:11	0.51[a]
	Age (years)	29.1(7.57)	28.75 (9.07)	0.89[b]
	Education (years)	16.95 (2.74)	15.45 (2.23)	0.06[b]
IQ	KBIT	108.11 (7.23)	104.75 (26.59)	0.60[b]
Language	BEST Spanish PN (%)	99.76 (0.56)	99.84 (0.47)	0.64[b]
	BEST Spanish INT	5 (0)	5 (0)	–
	LexTALE Spanish	94.75 (5.43)	92.62 (5.86)	0.24[b]
	BEST Basque PN (%)	90.53 (9.16)	37 (11.37)	**< 0.0001**[b]
	BEST Basque INT	4.95 (0.08)	1.92 (0.87)	**< 0.0001**[b]
	LexTALE Basque	87.5 (8.66)	32.2 (16.21)	**< 0.0001**[b]
	AoA Spanish	0.55 (1.39)	0	0.085[b]
	AoA Basque	1 (1.62)	–	

Note: Sex data are presented as males:females. Bold *p*-values indicate statistical significance.

Abbreviations: AoA, age of acquisition; BEST, Basque, English, and Spanish Test; INT, interview; IQ, intellectual quotient; KBIT, Kaufman Brief Intelligence Test; PN, picture-naming.

[a]*p*-value obtained via a chi-squared test.

[b]*p*-value obtained through two-tailed unpaired *t*-tests.

right-handed as defined by the Edinburgh Inventory,[27] and possessed normal or corrected-to-normal vision. None of them reported past neurological or psychiatric history. The two groups were matched for sex, age, years of education, and intellectual abilities via the Kaufman Brief Intelligence Test.[28]

All bilinguals had acquired their languages by the age of 5, and used them both on a daily basis. Conversely, monolinguals used only Spanish and had little to null knowledge of Basque. Language proficiency was objectively measured with the first and second parts of the BEST test.[29] The first part requires participants to name 65 pictures in their two languages, with scores ranging from 0 to 65. The second part consists of a semi-structured interview that measures fluency, lexical resources, grammatical constructions, and pronunciation via means of a Likert-like scale with scores ranging from 1 to 5. All highly proficient bilinguals scored above the cutoff for high proficiency in the first (≥ 70%) and second parts (≥ 4) of the BEST in both languages, while monolinguals met these criteria for Spanish but scored below it for Basque (i.e., ≤ 45% and ≤ 2, respectively). Participants also completed a Spanish[30] and a Basque version[29] of the LexTALE,[31] a short lexical decision test that provides good estimates of vocabulary knowledge in a given language. Briefly, participants were presented with 60 items (i.e., 40 words and 20 pseudo-words) and they were asked to indicate whether the item was an existing word or not. Descriptive and inferential statistics for each variable are shown in Table 1.

Before the experiment, all participants provided written informed consent. The study protocol was approved by the Ethics Committee of the Basque Center for Cognition, Brain, and Language (BCBL) and carried out in accordance with the Code of Ethics of the World Medical Association (Declaration of Helsinki).

MEG data acquisition

Figure 1 shows the study's pipeline. We followed current state-of-the-art guidelines[32,33] for MEG data acquisition, preprocessing, and analysis. MEG signals were acquired in a magnetically shielded room using a 306-channel Elekta Neuromag system. Signals were recorded at a 1 kHz sampling rate and filtered online at a bandwidth of 0.1–330 Hz. Data were obtained during an eyes-closed 5-min period in which participants were instructed not to think about anything in particular while keeping awake and still.

Participants' head position inside the helmet was continuously monitored using five head-position indicator coils. Six electrode pairs were used to measure horizontal and vertical ocular and cardiac activity. The standard fiducial landmarks (i.e., left and right preauricular points and nasion) plus ∼300 additional points registered over the scalp and eyes/nose contours were digitalized and used to spatially align the MEG sensor coordinates to the native T1 structural MRI of each participant. T1s were acquired with a Siemens 3T Magnetom Prisma Fit MR scanner in a separate session with the following parameters: echo time = 2.97 ms, nonswitching time = 2530 ms, flip angle = 7° and field of view = 256×256×176 mm^3, number of axial slices = 176, slice thickness = 1 mm, in-plane resolution = 1 mm × 1 mm.

MEG data preprocessing

Continuous data were preprocessed offline using the temporal extension of the signal space separation method[34] implemented in Maxfilter 2.2 (Elekta-Neuromag). Briefly, this method subtracts external magnetic noise from the MEG recordings, corrects for head movements, and interpolates bad/noisy channels. Subsequent analyses were
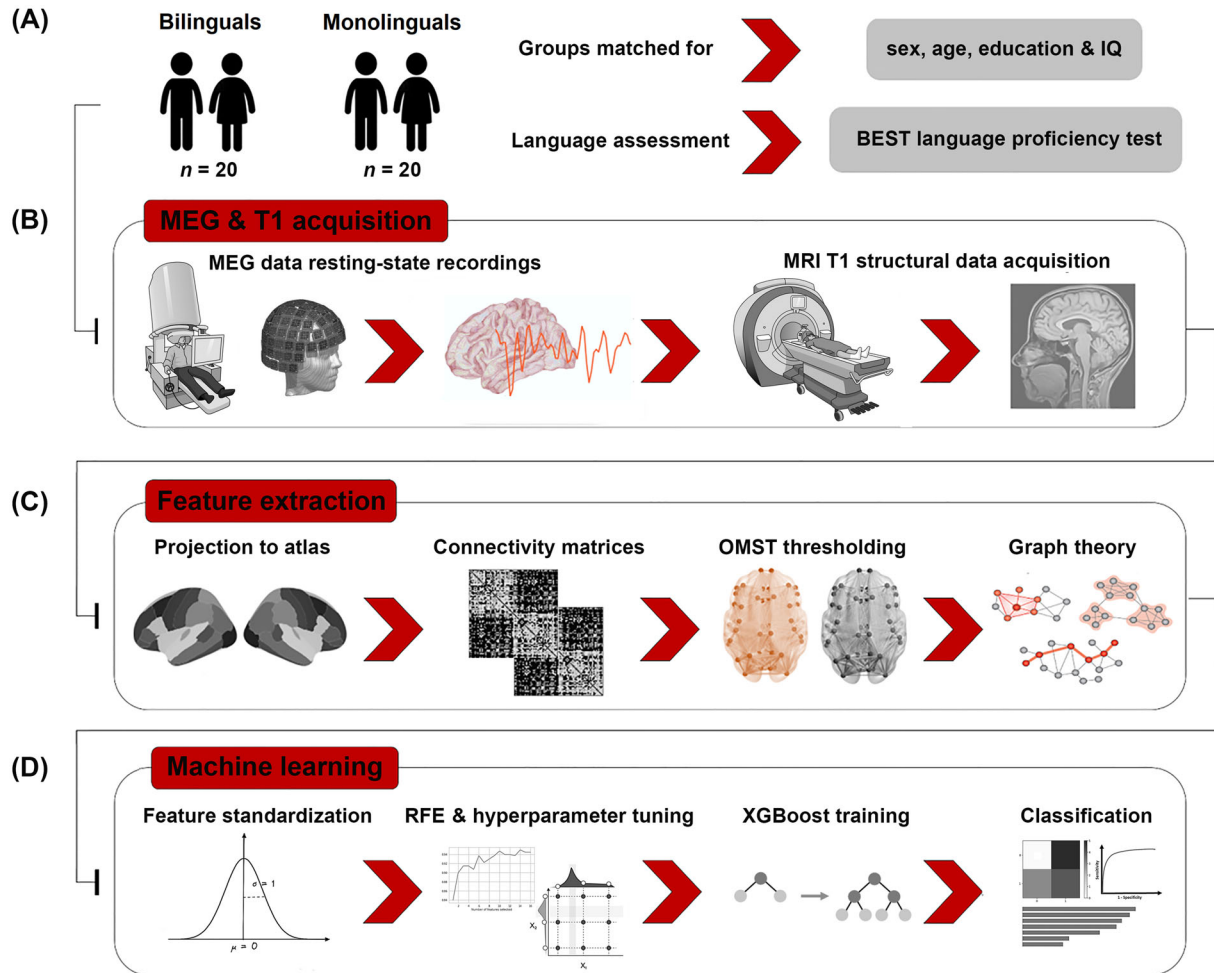
FIGURE 1 Preprocessing, data analysis, and machine learning pipeline. (A) Samples and neuropsychological assessment. Highly proficient bilinguals and monolinguals were matched for demographic variables (sex, age, education) and IQ. Language proficiency measures were acquired via means of the BEST test. (B) MEG and structural data acquisition. MEG activity was recorded under wakeful rest. (C) Data processing and connectivity analysis. We employed a source-based approach to connectivity. We estimated MEG sources using MNE and projected activity onto the 68 anatomical regions of the Desikan–Killiany atlas. Source-based whole-brain connectivity was calculated using the imaginary part of coherency (iCOH) in the delta (2–4 Hz), theta (4–8 Hz), alpha (8–12 Hz), beta (15–30 Hz), and gamma (30–80 Hz) bands. Adjacency matrices were filtered with the orthogonal minimal spanning trees method. Finally, graph theory measures were estimated from resting-state data at the different frequency-bands and fed into a machine learning classifier. (D) Machine learning pipeline. After feature standardization, we used recursive feature elimination with cross-validation (RFECV) and a grid search scheme for hyperparameter tuning to obtain trained XGBoost models. Then, we tested classification by employing the ROC-AUC, confusion matrices, and a feature importance analysis based on SHAP values. Abbreviations: BEST, Basque, English, and Spanish Test; MEG, magnetoencephalography; OMST, orthogonal minimal spanning trees; RFE, recursive feature elimination; ROC-AUC, receiver operating characteristic–area under the curve; SHAP, SHapley Additive exPlanations.

performed using the Brainstorm toolbox.[35] Signals were down-sampled offline to 500 Hz. Next, we applied a notch filter to eliminate powerline signal contamination at 50 Hz. MEG data containing non-stereotyped artifacts (e.g., jumps) were manually removed by visual inspection based on their time series and activation spectra. On the other hand, MEG data containing stereotyped artifacts (e.g., muscular, cardiac, and blinks) were retained. Independent component analysis[36] was applied in order to isolate and remove these physiological artifacts. Removed components ranged from one to four per participant. Next, following standard practice to capture data variance,[33] clean resting-state recordings were segmented into 4-s segments. After data cleaning, ∼80% of the segments remained per participant, with non-

significant differences ($p = 0.67$) between groups (bilinguals: $M = 67.65$, $SD = 5.22$; monolinguals: $M = 68.6$, $SD = 8.55$).

MEG source modeling

We used a source-based connectivity approach. To estimate the neural MEG sources, we selected 68 anatomical regions of interest (ROIs) from the Desikan–Killiany atlas.[37] Individual high-resolution 3D structural T1 MRIs were segmented through Freesurfer software.[38] The registration between the participant's MRI and the MEG was done automatically using Brainstorm based on the fiducials and the

additional 300 digitalized head points. The MEG forward model was computed using the overlapping-spheres approach.[39] Next, the noise covariance matrix was calculated from empty-room recordings (∼3–5 min), in order to characterize instrument and environmental noise. The solution space was constrained to the cerebral cortex which was modeled as a three-dimensional grid of 15,000 fixed dipoles oriented normally to the cortical surface. Then, the inverse solution was estimated with the weighted minimum norm estimation.[40] Finally, the time series from the 68 ROIs were estimated as the average of all dipole's signals within each area.

MEG functional connectivity

The imaginary part of coherency (iCOH) was used to measure rsFC between all 68 ROIs in canonical frequency bands, namely: delta (2–4 Hz), theta (4–8 Hz), alpha (8–12 Hz), beta (15–30 Hz), and gamma (30–80 Hz). The use of iCOH was originally proposed[41] to overcome volume conduction problems when estimating FC in MEG data. The iCOH is sensitive only to the synchronization of two processes that are time-lagged to each other. Since volume conduction does not cause a time-lag, the iCOH is insensitive to spurious interactions. Using the iCOH, the zero-lag effect can be suppressed, because the real part is the one mostly affected by this aspect. The iCOH was calculated according to Equation (1):

$$I_{xy}(f) = \left| Im \frac{\sum_{k=1}^{k} X_k(f) Y_k^*(f)}{\sqrt{\sum_{k=1}^{k} |X_k(f)|^2 \sum_{k=1}^{k} |Y_k(f)|^2}} \right|, \tag{1}$$

where $I_{xy}(f)$ is the imaginary coherence between a given pair of ROIs for each frequency, Im is the imaginary part of the complex production, X_k and Y_k are the source-based spectrums from the two ROIs, * denotes the complex conjugate, and K is the number of 4-s length segments.

Adjacency matrices were filtered using the orthogonal minimal spanning trees (OMST) algorithm.[42] OMST is a novel data-driven topological thresholding technique that maximizes the information flow over the network versus the cost. Briefly, this method samples the full-weighted matrix over successive rounds of minimum spanning trees that are orthogonal to each other, identifying essential connections via optimizing the global efficiency of the network constrained by the cost of surviving connections.[43] This method outperforms conventional approaches in capturing MEG resting-state networks' most essential connections.[42]

Graph-theory metrics

The architecture of participants' resting-state networks was characterized via graph-theory metrics[24] in the Brain Connectivity Toolbox.[44] Based on previous bilingualism research,[45–47] we selected eight measures broadly capturing global and local aspects of the networks'

organization, each defined in Table 2. These metrics were computed for each frequency band (i.e., delta, theta, alpha, beta, and gamma), yielding 40 features per participant.

Machine learning analysis

We employed a binary classification machine learning approach to distinguish between bilingual and monolingual individuals based on spectral topological features derived from rsFC. To achieve this, we utilized the Extreme Gradient Boosting (XGBoost) algorithm, a powerful ensemble method that combines individually weak yet complementary classifiers to construct a robust estimator.[48] This algorithm incorporates regularization in its boosting process, thus mitigating overfitting and enhancing the generalizability of the results. Recognized for its outstanding performance and speed, XGBoost has become a dominant algorithm in applied machine learning.[49] A recent state-of-the-art comparison of classification algorithms[50] underscores XGBoost's effectiveness across both small and large training sets— consistently outperforming more popular classifiers such as support vector machine and random forest.

First, we applied feature standardization using the robust scaler method. This technique involves calculating the median alongside the 25th and 75th percentiles for each feature. Subsequently, the values of each feature undergo a transformation where the median is subtracted, and the result is divided by the interquartile range. The outcome is a standardized variable with a zero mean and median, and a standard deviation of 1. This robust method ensures the resulting features remain resilient to the influence of outliers, maintaining their stability even in the presence of skewed data.

Subsequently, we implemented a nested cross-validation strategy (outer loop: k-fold = 10; inner loop: k-fold = 5).[51] The dataset was randomly partitioned into different train-test splits, with each run utilizing nine folds for training and reserving one (hold-out) fold for testing. Within each outer fold, an inner loop was executed to perform feature reduction through recursive feature elimination with cross-validation[52,53]; and hyperparameter tuning using the Grid Search method.[54] The model was then trained with the best hyperparameters and the reduced set of features. Importantly, the participant-to-feature ratio met the recommended N-1 criterion across all runs (mean number of features = 10; range: 5–19), where N denotes the number of subjects used in the training set.[55] This dual optimization within the inner loop ensured that features and hyperparameters were tailored to the specific characteristics of each training set, preventing overfitting, and yielding a more generalized model.

In keeping with current guidelines to report machine learning results,[56] classification performance was evaluated using the area under the curve (AUC) of the receiver operating characteristic (ROC) curve, accuracy, sensitivity, specificity, and F1-scores. Mean and standard deviation values across folds were reported for each metric. To identify the most predictive variables, we calculated absolute SHAP (SHapley Additive exPlanations) values[57,58] and examined the impact of each feature on the model's predictions throughout every

TABLE 2   Global and local aspects of networks' organization.

Graph theory metric	Definition
Global measures	
Characteristic path length (CPL)	Average shortest path length between all pairs of nodes in the network. This metric captures functional integration in brain networks.
Global efficiency (GE)	Average inverse shortest path length in the network. It captures the efficiency of distant information transfer in a given network.
Average node strength (ANS)	Arithmetic average of the strengths of all the individual nodes in the network. It represents the sum of all incoming and outgoing edge weights. This metric quantifies global degree of connectivity.
Small-worldness index (*Sw*)	Characterization of a network's architecture, usually determined by low average path length and high clustering. Small-world networks are a "middle-ground" between random and regular networks. This property has the lowest wiring costs, the most efficient information transfer, and the best balance of local and global information. We computed this index as defined by Humphries and Gurney (2008),[91] in which a network is deemed a "small-world" if $Sw > 1$.
Local measures	
Clustering coefficient (C)	Number of connections between a node's nearest neighbors, calculated as a ratio of the maximum number of possible connections. This metric captures the level of local connectedness of a network.
Local efficiency (LE)	GE as computed in the neighborhood of the node. This metric estimates communication efficiency between a node's neighbors.
Betweenness centrality (BC)	Quantification of how many of the shortest paths between all other node pairs in the network pass through a given node. This metric shows which nodes act as bridges between nodes, detecting how much a node influences information flow in a given network.
Participation coefficient (PC)	Typically interpreted as an index of a region's "hubness." Captures the diversity of a node's links across network communities. This metric reveals how well a node integrates information and coordinates connectivity between communities.

iteration. These absolute SHAP values were then aggregated across folds, yielding a comprehensive matrix that captured the nuanced influence of features on the model's decision-making. Specifically, we focused on the top 10 features with the highest mean absolute importance across folds, providing an insightful summary of the most influential contributors to the model's discriminatory prowess. All analyses were implemented using the Scikit-learn library (v. 0.22.1) in Python.

Statistical network analysis

To further characterize differences between bilinguals and monolinguals in global network topology, we determined the direction of between-group effects on the top-ranked features highlighted by the machine learning analysis using Mann–Whitney U tests (two-tailed). Subsequently, we investigated hub regions within these networks using individual nodal strength. For each participant, nodal strength was calculated as the sum of the weights of its connections with the rest of the nodes. This metric serves as a robust indicator of the influence or communicational importance of individual regions within a network.[59] The 68 anatomical ROIs of the Desikan–Killiany atlas were used as nodes. We then employed Mann–Whitney U tests to compare differences between groups, considering each node separately and applying false discovery rate (FDR) correction for multiple comparisons,[60] at an alpha level = 0.05. Specifying influential nodes provides a more fine-grained understanding of key regions driving whole-brain effects,

thereby improving the interpretation of the canonical networks that could be involved (e.g., salience, default-mode network [DMN]). Importantly, the use of both global and nodal metrics is a well-established practice in network analysis.[25,61–63]

Correlation analysis

We employed a correlational analysis to further test for the robustness of our data-driven approach. Using the Robust Correlation Toolbox[64] in MATLAB R2012B, we examined potential associations between top-ranked features and bilinguals' L2 proficiency (i.e., BEST and Lex-TALE scores in Basque). We employed percentage-bend correlations,[65] known for providing an accurate estimate of the true relationship between two variables, while protecting against marginal outliers.

RESULTS

Machine learning results

The machine learning classifier yielded an AUC of 0.91 ($\pm$ 0.12), with an accuracy of 84.8% ($\pm$ 5%), a sensitivity of 83.3% ($\pm$ 25.8%), a specificity of 76.7% ($\pm$ 32%), and an F1-score of 0.78 $\pm$ 0.19 (Figure 2). Estimates of feature importance using SHAP values highlighted ANS in beta and delta as the top-ranked features determining compound classification in our model.
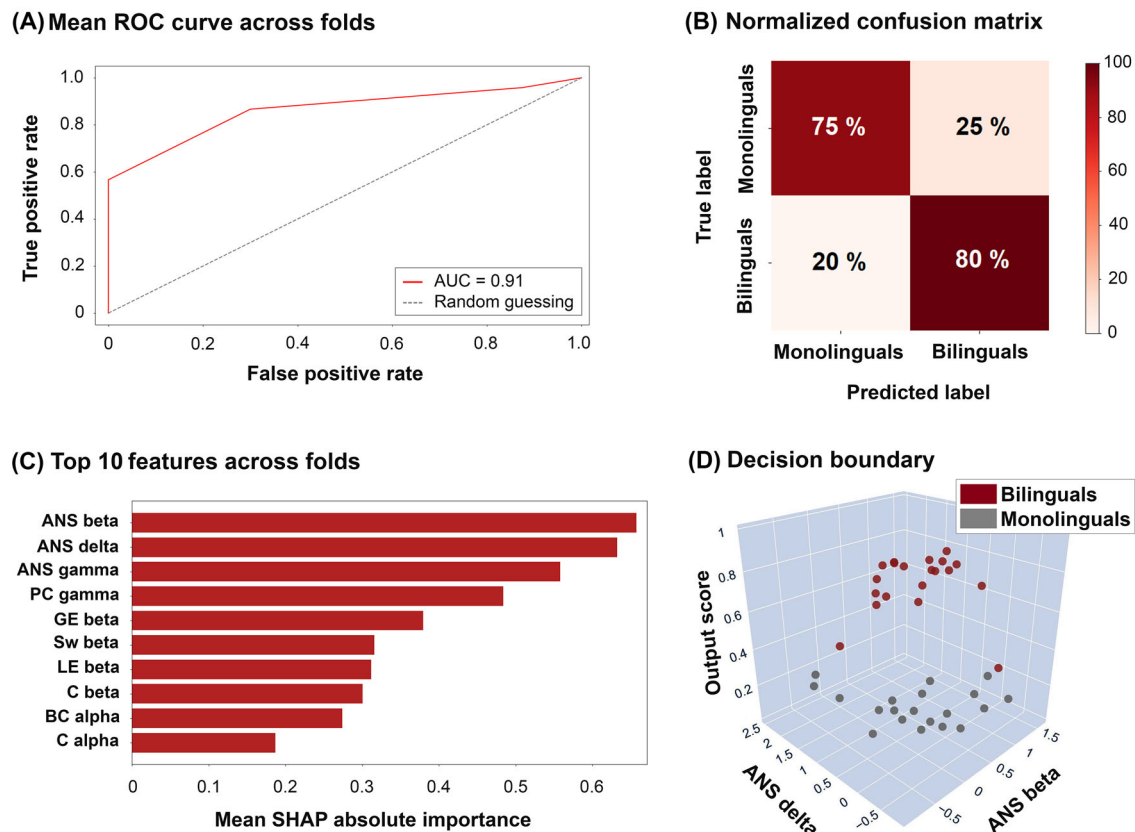
FIGURE 2 Machine learning results. (A) Area under receiver operating characteristic (ROC) curve (AUC) and (B) confusion matrix of the classification model. (C) List of the top 10 most predictive features across folds (in order of importance), using absolute SHAP values. (D) Output scores based on the two top-ranked features revealed excellent detection of bilingual and monolingual individuals using a decision boundary of 0.5. Final output score per participant was obtained after averaging it over 1000 iterations. Abbreviations: ANS, average node strength; BC, betweenness centrality; C, clustering coefficient; GE, global efficiency; LE, local efficiency; PC, participation coefficient; SHAP, SHapley Additive exPlanations; SW, small-worldness index.

Statistical network results

ANS in beta ($U = 102$, $Z = 2.63$, $p = 0.007$; RBC = −0.49) and delta ($U = 104$, $Z = 2.58$, $p = 0.009$; RBC = −0.48) rhythms were significantly lower for bilinguals compared to monolinguals (Figure 3A). When considering individual node strength (Figure 3B), influential regions differing between groups in the beta band involved the left middle frontal gyrus (MFG); the left temporal pole (TPO), middle (MTG), and superior temporal gyri (STG); and the right insula (INS), posterior cingulate cortex (PCC), postcentral gyrus (PoCG), parahippocampal gyrus (PHG), and inferior parietal lobe (IPL). The delta band spanned the bilateral fusiform gyri (FFG) and orbitofrontal cortices (OFC); the left PCC and superior parietal lobe (SPL); and the right anterior cingulate (ACC) and supramarginal gyrus (SMG).

Correlation results

This analysis yielded significant negative correlations between ANS in beta and LexTALE L2 scores (Bend $r = −0.53$, $p = 0.01$) and between ANS in delta and BEST L2 scores (Bend $r = −0.46$, $p = 0.04$). Scatter-

plots showing associations between these features with LexTALE and BEST scores in Basque are provided in Figure 3C.

DISCUSSION

Can lifelong bilingualism be robustly decoded from the organization of oscillatory resting-state networks? To answer this question, we recoded task-free MEG activity from highly proficient bilinguals and monolinguals, derived topological network properties in canonical frequency bands, and trained a machine learning classifier to predict individuals' dual-language experience. Overall, the model achieved an excellent performance (AUC: 0.91 ± 0.12) in distinguishing between individuals at a probabilistic subject-level. The classification was mainly driven by network strength in the beta (15–30 Hz) and delta (2–4 Hz) bands, involving temporal, cingulate, and fronto-parietal hubs. These features also correlated with L2 proficiency in bilinguals, further validating our automated multivariate approach.

Previous evidence indicates that L2 acquisition has a significant impact on the organization of intrinsic brain networks. However, most existing studies rely on fMRI rsFC, which is blind to the full

(A) Network strength differences between groups
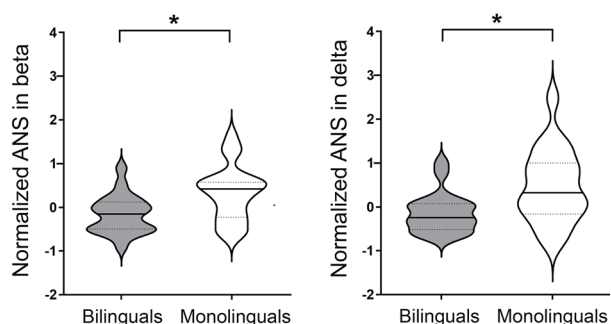
(B) Node strength differences between groups

Beta (15-30 Hz)

Delta (2-4 Hz)
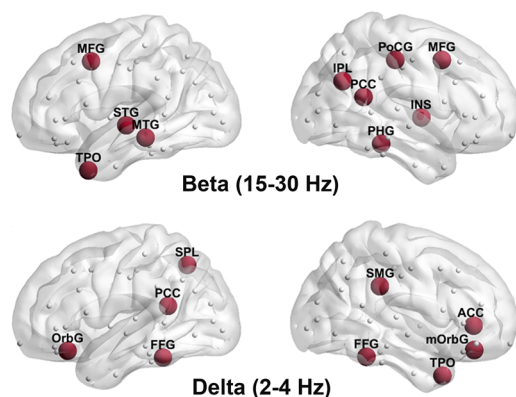
(C) Correlations with L2 proficiency in bilinguals
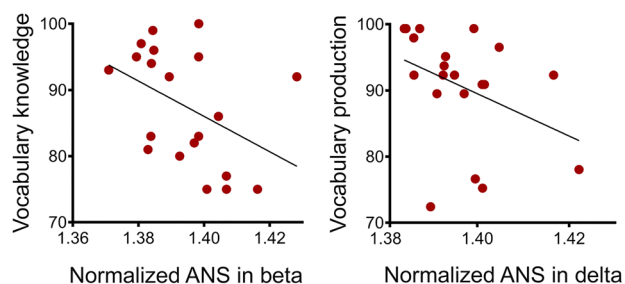
FIGURE 3 Resting-state network differences between highly proficient bilinguals and monolinguals. (A) Violin plots showing total weight (ANS) significant differences between groups in beta (15–30 Hz) and delta (2–4 Hz) frequency bands. Straight lines within the violin plots indicate the median and dotted lines the interquartile range. (B) Spatial distribution of the brain network nodes showing maximal strength difference between groups in beta and delta rhythms. Only significant (FDR-corrected p-values < 0.05) nodes are plotted. (C) Scatterplots showing relationships between top-ranked resting-state oscillatory features (ANS in beta and delta) and measures of L2 (Basque) proficiency. Abbreviations: ACC, anterior cingulate cortex; ANS, average node strength; FFG, fusiform gyrus; INS, insula; IPL, inferior parietal lobe; MFG, middle frontal gyrus; MTG, middle temporal gyrus; OFC, orbitofrontal cortex; PCC, posterior cingulate cortex; PHG, parahippocampal gyrus; PoCG, postcentral gyrus; SMG, supramarginal gyrus; SPL, superior parietal lobe; STG, superior temporal gyrus; TPO, temporal pole.

spectral richness of brain signals. By using a spectrally resolved decoding approach, we show that global strength in beta and delta rhythms robustly classified individuals based on their dual-language background. These findings align with previous studies conducted in other domains of expertise, such as the acquisition of sensorimotor skills in elite gymnasts[66] and professional dancers,[25] where global measures successfully classified participants based on prior experience. Notably, in these studies, global topological properties were lower in experts as compared to nonexperts, a finding that mirrors our results and likely reflects a greater level of automaticity and efficiency resulting from long-term training or exposure in a particular domain. Similarly, in bilinguals, critical hubs become more selectively coupled with a subset of other brain regions, albeit at the expense of lower (unspecific) coupling at the whole-brain level.[67] Overall, this suggests that lifelong experience with sociocognitive skills consistently shapes the brain across individuals, underscoring the significance of beta and delta oscillations in capturing these effects within the bilingual domain.

Consistent with our hypothesis, global beta strength emerged as the most influential feature in distinguishing bilinguals from monolinguals. This aligns with prior evidence showing that rsFC in this specific frequency band is modulated by the degree of dual-language experience[17,19] and can successfully predict (~60%) the variability in L2 learning rates following intensive training.[20,21] Additionally, the node-based analysis identified key regions exhibiting greater connectivity differences in the beta network, primarily involving language-specific nodes in the temporal lobe. These nodes include the middle and superior temporal gyrus, the temporal pole, and the parahippocampal gyrus, which have been widely implicated in lexico-semantic processes, including lexical access and the retrieval of conceptual knowledge from long-term memory.[68–70] Moreover, there is evidence indicating that beta rhythms support the reallocation of linguistic functions in bilingual patients with brain damage.[71] Thus, this finding suggests that bilingual experience impacts the topological organization of brain networks dedicated to language-specific functions.

Whole-network delta strength emerged as the second most influential feature in distinguishing individuals within each group. Slow delta oscillations play a crucial role in the brain's ability to integrate information across large-scale networks,[72] facilitating macroscale interactions. Synchronous delta activity in fronto-parietal and cingulate cortices has been linked to cognitive control in the general population[73] and to language switching in bilinguals.[74,75] This aligns with the significant nodes captured by our node-level analysis, including bilateral parietal cortices, anterior and posterior cingulate areas, and orbitofrontal regions. Notably, several of these nodes also overlap with central hubs of the DMN,[76] a set of regions that deactivate during tasks and have been recently proposed to orchestrate the recruitment of different brain systems that underpin cognition.[77,78] Additional support for this interpretation comes from studies showing a strong link between rsFC in the DMN and delta oscillations,[79,80] with variations in intrinsic DMN connectivity being significantly explained by synchronization in this slow brain rhythm. Hence, this top-ranked feature may reflect the influence of bilingualism on a network that forms the backbone for global brain communication at

rest. This finding holds particular relevance as previous M/EEG studies investigating rsFC in bilinguals have systematically neglected the analysis of delta rhythms due to artifact-related issues during data acquisition.[17,19,20]

Moreover, the correlation analysis demonstrated that the top-ranked features, namely, beta and delta global strength, explained interindividual variability in L2 proficiency among bilinguals. Specifically, lower beta and delta strength were associated with higher L2 proficiency in vocabulary knowledge (LexTALE) and language production (BEST) measures, respectively. These findings are consistent with previous evidence indicating that higher rates of vocabulary learning correlate with beta power modulations.[81] Additionally, better performance in picture-naming negatively correlates with rsFC in the DMN,[82,83] as indexed here by delta dynamics. Furthermore, in the bilingual domain, beta[20,21] and delta[84] connectivity have been shown to correlate with L2 learning proficiency. Importantly, our study extends this evidence beyond early (transient) training effects to sustained lifelong experience with an L2, suggesting that the impact of bilingualism on beta and delta networks persists throughout continuous language use.

Our findings have important theoretical implications and introduce a new (spectral) dimension to current models of bilingualism, which traditionally focused on rsFC differences between brain regions. First, by delving into oscillatory topological signatures, we offer insights into how these brain regions bind together and communicate within specific frequency bands—an approach proven fruitful in modeling lifelong expertise in other domains.[25] Second, unlike prior studies overlooking interindividual variability in spectral profiles, our multivariate approach demonstrates that dual-language expertise can be robustly decoded from connectome-like MEG information at the probabilistic subject level. This allows for predicting an individual's bilingual status solely from intrinsic brain activity, underscoring that the resting-state dynamics of the bilingual brain consistently differ from those of monolinguals. This perspective aligns well with the spontaneous trait reactivation hypothesis,[85] wherein the organization of the human brain at rest provides insight into the individual's distinctive traits and abilities.[86] Third, our findings contribute to characterizing the direction of bilingual experience effects on rsFC—a topic of interest due to contradictory findings.[87] We show that bilinguals exhibit decreased connectivity strength in specific oscillatory networks within the beta and delta bands, and that this reduction correlates with higher proficiency in the L2. This association may indicate a more efficient and automatic recruitment of brain functions in bilinguals resulting from sustained learning, as observed in other expertise domains.[25,66,88]

Overall, our results suggest that the compound classification between bilinguals and monolinguals is probably rooted in neuroplastic changes occurring within two key networks: the language network, characterized by beta patterns; and the DMN, characterized by delta patterns. These networks play a central role in lexico-semantic processing and in orchestrating cognition. Thus, our study provides valuable insights into the neural effects of bilingualism on high-level human functions, addressing the call for a more nuanced understanding of these phenomena.

Nevertheless, there are some limitations to the current study. First, our sample size was relatively small, although comparable to those reported in similar studies using oscillatory features for binary classification of individuals with varying degrees of sociocognitive skills[25] and learning styles.[89] Second, our findings are restricted to Spanish-Basque bilinguals and future studies should investigate whether they can be generalized to speakers of other languages. Lastly, the age range of our sample was restricted to young adults, while it is known that FC can be altered by aging.[26,90] Consequently, it is crucial to explore in future research whether our findings can be extended to other age cohorts.

CONCLUSION

Our study provides compelling evidence that lifelong bilingualism involves reconfigurations of specific oscillatory networks, leaving a pervasive imprint that can be robustly decoded even at rest. Moreover, we show that beta and delta strength can serve as potential markers of L2 proficiency, effectively capturing interindividual differences in dual-language experience. Overall, these findings underscore the significance of frequency-specific oscillatory networks in unraveling the neural signatures of bilingualism.

AUTHOR CONTRIBUTIONS

L.A.: Conceptualization; methodology; formal analysis; writing original draft; reviewing and editing and supervision. A.M.G.: Conceptualization; reviewing and editing. S.P.: Data curation; investigation; methodology; formal analysis. I.Q.: Investigation; methodology; reviewing and editing. P.T.: Data curation; investigation; resources. M.C.: Conceptualization; writing reviewing and editing; supervision.

COMPETING INTERESTS

The authors declare no competing interests.

DATA AVAILABILITY STATEMENT

The data and scripts that support the findings of this study are available at https://osf.io/gu597/.

ORCID

Lucia Amoruso https://orcid.org/0000-0003-4696-2187

PEER REVIEW

The peer review history for this article is available at: https://publons.com/publon/10.1111/nyas.15113.

REFERENCES

1. Kroll, J. F., Dussias, P. E., Bice, K., & Perrotti, L. (2015). Bilingualism, mind, and brain. *Annual Review of Linguistics*, 1, 377–394.
2. Maguire, E. A., Gadian, D. G., Johnsrude, I. S., Good, C. D., Ashburner, J., Frackowiak, R. S., & Frith, C. D. (2000). Navigation-related structural change in the hippocampi of taxi drivers. *Proceedings of the National Academy of Sciences of the United States of America*, 97(8), 4398–4403.
3. Shen, H., Li, Z., Qin, J., Liu, Q., Wang, L., Zeng, L. L., Li, H., & Hu, D. (2016). Changes in functional connectivity dynamics associated with vigilance network in taxi drivers. *Neuroimage*, 124, (Pt A), 367–378.
4. Pinho, A. L., de Manzano, O., Fransson, P., Eriksson, H., & Ullen, F. (2014). Connecting to create: Expertise in musical improvisation is associated with increased functional connectivity between premotor and prefrontal areas. *Journal of Neuroscience*, 34(18), 6156–6163.
5. Draganski, B., Gaser, C., Busch, V., Schuierer, G., Bogdahn, U., & May, A. (2004). Neuroplasticity: Changes in grey matter induced by training. *Nature*, 427(6972), 311–312.
6. Amoruso, L., Ibanez, A., Fonseca, B., Gadea, S., Sedeno, L., Sigman, M., García, A. M., Fraiman, R., & Fraiman, D. (2017). Variability in functional brain networks predicts expertise during action observation. *Neuroimage*, 146, 690–700.
7. Li, P., Legault, J., & Litcofsky, K. A. (2014). Neuroplasticity as a function of second language learning: Anatomical changes in the human brain. *Cortex*, 58, 301–324.
8. García-Pentón, F. G. Y., Costello, B., Duñabeitia, J. A., & Carreiras, M. (2016). The neuroanatomy of bilingualism: How to turn a hazy view into the full picture. *Language, Cognition and Neuroscience*, 31(3), 303–327.
9. Sulpizio, S., sel Maschio, N., Del Mauro, G., Fedeli, D., & Abutalebi, J. (2020). Bilingualism as a gradient measure modulates functional connectivity of language and control networks. *Neuroimage*, 205, 116306.
10. Berken, J. A., Chai, X., Chen, J. K., Gracco, V. L., & Klein, D. (2016). Effects of early and late bilingualism on resting-state functional connectivity. *Journal of Neuroscience*, 36(4), 1165–1172.
11. Grady, C. L., Luk, G., Craik, F. I., & Bialystok, E. (2015). Brain network activity in monolingual and bilingual older adults. *Neuropsychologia*, 66, 170–181.
12. Gullifer, J. W., Chai, X. J., Whitford, V., Pivneva, I., Baum, S., Klein, D., & Titone, D. (2018). Bilingual experience and resting-state brain connectivity: Impacts of L2 age of acquisition and social diversity of language use on control networks. *Neuropsychologia*, 117, 123–134.
13. DeLuca, V., Rothman, J., Bialystok, E., & Pliatsikas, C. (2019). Redefining bilingualism as a spectrum of experiences that differentially affects brain structure and function. *Proceedings of the National Academy of Sciences of the United States of America*, 116(15), 7565–7574.
14. Tao, L., Wang, G., Zhu, M., & Cai, Q. (2021). Bilingualism and domain-general cognitive functions from a neural perspective: A systematic review. *Neuroscience and Biobehavioral Reviews*, 125, 264–295.
15. Lewis, L. D., Setsompop, K., Rosen, B. R., & Polimeni, J. R. (2016). Fast fMRI can detect oscillatory neural activity in humans. *Proceedings of the National Academy of Sciences of the United States of America*, 113(43), E6679–E6685.
16. Buzsaki, G., & Draguhn, A. (2004). Neuronal oscillations in cortical networks. *Science*, 304(5679), 1926–1929.
17. Bice, K., Yamasaki, B. L., & Prat, C. S. (2020). Bilingual language experience shapes resting-state brain rhythms. *Neurobiology of Language*, 1(3), 288–318.
18. de Frutos-Lucas, J., López-Sanz, D., Cuesta, P., Bruña, R., de la Fuente, S., Serrano, N., & Maestú, F. (2019). Enhancement of posterior brain functional networks in bilingual older adults. *Bilingualism: Language and Cognition*, 23(2), 387–400.
19. Pereira Soares, S. M., Kubota, M., Rossi, E., & Rothman, J. (2021). Determinants of bilingualism predict dynamic changes in resting state EEG oscillations. *Brain and Language*, 223, 105030.
20. Prat, C. S., Yamasaki, B. L., Kluender, R. A., & Stocco, A. (2016). Resting-state qEEG predicts rate of second language learning in adults. *Brain and Language*, 157-158, 44–50.
21. Prat, C. S., Yamasaki, B. L., & Peterson, E. R. (2019). Individual differences in resting-state brain rhythms uniquely predict second language learning rate and willingness to communicate in adults. *Journal of Cognitive Neuroscience*, 31(1), 78–94.
22. Kussner, M. B., de Groot, A. M., Hofman, W. F., & Hillen, M. A. (2016). EEG beta power but not background music predicts the recall scores in a foreign-vocabulary learning task. *PLoS ONE*, 11(8), e0161387.
23. Kliesch, M., Giroud, N., & Meyer, M. (2021). EEG resting-state and event-related potentials as markers of learning success in older adults following second language training: A pilot study. *Brain Plasticity*, 7(2), 143–162.
24. Bullmore, E., & Sporns, O. (2009). Complex brain networks: Graph theoretical analysis of structural and functional systems. *Nature Reviews Neuroscience*, 10(3), 186–198.
25. Amoruso, L., Pusil, S., Garcia, A. M., & Ibanez, A. (2022). Decoding motor expertise from fine-tuned oscillatory network organization. *Human Brain Mapping*, 43(9), 2817–2832.
26. Kliesch, M., Becker, R., & Hervais-Adelman, A. (2022). Global and localized network characteristics of the resting brain predict and adapt to foreign language learning in older adults. *Scientific Reports*, 12(1), 3633.
27. Oldfield, R. C. (1971). The assessment and analysis of handedness: The Edinburgh inventory. *Neuropsychologia*, 9(1), 97–113.
28. Kaufman, A. S., & Kaufman, N. L. (2004). *Kaufman Brief Intelligence Test*.
29. de Bruin, A., Carreiras, M., & Dunabeitia, J. A. (2017). The BEST dataset of language proficiency. *Frontiers in Psychology*, 8, 522.
30. Izura, C. C. F., & Brysbaert, M. (2014). Lextale-Esp: A test to rapidly and efficiently assess the Spanish vocabulary size. *Psicológica*, 35, 49–66.
31. Lemhofer, K., & Broersma, M. (2012). Introducing LexTALE: A quick and valid lexical test for advanced learners of English. *Behavior Research Methods*, 44(2), 325–343.
32. Gross, J., Baillet, S., Barnes, G. R., Henson, R. N., Hillebrand, A., Jensen, O., Jerbi, K., Litvak, V., Maess, B., Oostenveld, R., Parkkonen, L., Taylor, J. R., van Wassenhove, V., Wibral, M., & Schoffelen, J.-M. (2013). Good practice for conducting and reporting MEG research. *Neuroimage*, 65, 349–363.
33. Niso, G., Tadel, F., Bock, E., Cousineau, M., Santos, A., & Baillet, S. (2019). Brainstorm pipeline analysis of resting-state data from the open MEG archive. *Frontiers in Neuroscience*, 13, 284.
34. Taulu, S., & Simola, J. (2006). Spatiotemporal signal space separation method for rejecting nearby interference in MEG measurements. *Physics in Medicine and Biology*, 51(7), 1759–1768.

35. Tadel, F., Baillet, S., Mosher, J. C., Pantazis, D., & Leahy, R. M. (2011). Brainstorm: A user-friendly application for MEG/EEG analysis. *Computational Intelligence and Neuroscience*, *2011*, 879716.

36. Bell, A. J., & Sejnowski, T. J. (1995). An information-maximization approach to blind separation and blind deconvolution. *Neural Computation*, *7*(6), 1129–1159.

37. Desikan, R. S., Segonne, F., Fischl, B., Quinn, B. T., Dickerson, B. C., Blacker, D., Buckner, R. L., Dale, A. M., Maguire, R. P., Hyman, B. T., Albert, M. S., & Killiany, R. J. (2006). An automated labeling system for subdividing the human cerebral cortex on MRI scans into gyral based regions of interest. *Neuroimage*, *31*(3), 968–980.

38. Dale, A. M., & Sereno, M. I. (1993). Improved localizadon of cortical activity by combining EEG and MEG with MRI cortical surface reconstruction: A linear approach. *Journal of Cognitive Neuroscience*, *5*(2), 162–176.

39. Huang, M. X., Mosher, J. C., & Leahy, R. M. (1999). A sensor-weighted overlapping-sphere head model and exhaustive head model comparison for MEG. *Physics in Medicine and Biology*, *44*(2), 423–440.

40. Hamalainen, M. S., & Ilmoniemi, R. J. (1994). Interpreting magnetic fields of the brain: Minimum norm estimates. *Medical & Biological Engineering & Computing*, *32*(1), 35–42.

41. Nolte, G., Bai, O., Wheaton, L., Mari, Z., Vorbach, S., & Hallett, M. (2004). Identifying true brain interaction from EEG data using the imaginary part of coherency. *Clinical Neurophysiology*, *115*(10), 2292–2307.

42. Dimitriadis, S. I., Antonakakis, M., Simos, P., Fletcher, J. M., & Papanicolaou, A. C. (2017). Data-driven topological filtering based on orthogonal minimal spanning trees: Application to multigroup magnetoencephalography resting-state connectivity. *Brain Connectivity*, *7*(10), 661–670.

43. Stam, C. J. (2014). Modern network science of neurological disorders. *Nature Reviews Neuroscience*, *15*(10), 683–695.

44. Rubinov, M., & Sporns, O. (2010). Complex network measures of brain connectivity: Uses and interpretations. *Neuroimage*, *52*(3), 1059–1069.

45. Bilson, S., Yoshida, H., Tran, C. D., Woods, E. A., & Hills, T. T. (2015). Semantic facilitation in bilingual first language acquisition. *Cognition*, *140*, 122–134.

46. Borodkin, K., Kenett, Y. N., Faust, M., & Mashal, N. (2016). When pumpkin is closer to onion than to squash: The structure of the second language lexicon. *Cognition*, *156*, 60–70.

47. Ma, J., Fan, X., Pan, N., Xu, X., Jin, Y., Guo, X., Jing, J., & Li, X. (2022). The differences of functional brain network in processing auditory phonological tasks between Cantonese-Mandarin bilinguals and Mandarin monolinguals. *Brain Research*, *1780*, 147801.

48. Chen, T., & Guestrin, C. (2016). Xgboost: A scalable tree boosting system. In 22nd ACM SIGKDD International Conference on Knowledge Discovery and Data Mining. San Francisco, CA.

49. Uddin, S., Ong, S., & Lu, H. (2022). Machine learning in project analytics: A data-driven framework and case study. *Scientific Reports*, *12*(1), 15252.

50. Zhang, C., Liu, C., Zhang, X., & Almpanidis, G. (2017). An up-to-date comparison of state-of-the-art classification algorithms. *Expert Systems with Applications*, *82*, 128–150.

51. Chui, K. T., Liu, R. W., Zhao, M., & De Pablos, P. O. (2020). Predicting students' performance with school and family tutoring using generative adversarial network-based deep support vector machine. *IEEE Access*, *8*, 86745–86752.

52. Misra, P., & Yadav, A. S. (2020). Improving the classification accuracy using recursive feature elimination with cross-validation. *International Journal on Emerging Technologies*, *11*(3), 659–665.

53. Saeys, Y., Inza, I., & Larranaga, P. (2007). A review of feature selection techniques in bioinformatics. *Bioinformatics*, *23*(19), 2507–2517.

54. Pedregosa, F., Varoquaux, G., Gramfort, A., Michel, V., Thirion, B., Grisel, O., Blondel, M., Prettenhofer, P., Weiss, R., Dubourg, V., Vanderplas, J., Passos, A., Cournapeau, D., Brucher, M., Perrot, M., & Duchesnay, É. (2011). Scikit-learn: Machine learning in Python. *Journal of Machine Learning Research*, *12*, 2825–2830.

55. Hua, J., Xiong, Z., Lowey, J., Suh, E., & Dougherty, E. R. (2005). Optimal number of features as a function of sample size for various classification rules. *Bioinformatics*, *21*(8), 1509–1515.

56. Uddin, S., Khan, A., Hossain, M. E., & Moni, M. A. (2019). Comparing different supervised machine learning algorithms for disease prediction. *BMC Medical Informatics and Decision Making*, *19*(1), 281.

57. Lundberg, S. M., & Lee, S. (2017). A unified approach to interpreting model predictions. In Proceedings of the 31st International Conference on Neural Information Processing Systems (pp. 4768–4777).

58. Rodriguez-Perez, R., & Bajorath, J. (2020). Interpretation of compound activity predictions from complex machine learning models using local approximations and Shapley values. *Journal of Medicinal Chemistry*, *63*(16), 8761–8777.

59. Sporns, O. (2018). Graph theory methods: Applications in brain networks. *Dialogues in Clinical Neuroscience*, *20*(2), 111–121.

60. Hochberg, Y., & Benjamini, Y. (1990). More powerful procedures for multiple significance testing. *Statistics in Medicine*, *9*(7), 811–818.

61. Gonzalez-Burgos, L., Pereira, J. B., Mohanty, R., Barroso, J., Westman, E., & Ferreira, D. (2021). Cortical networks underpinning compensation of verbal fluency in normal aging. *Cerebral Cortex*, *31*(8), 3832–3845.

62. Vatansever, D., Schroter, M., Adapa, R. M., Bullmore, E. T., Menon, D. K., & Stamatakis, E. A. (2020). Reorganisation of brain hubs across altered states of consciousness. *Scientific Reports*, *10*(1), 3402.

63. Chino, B., Cuesta, P., Pacios, J., de Frutos-Lucas, J., Torres-Simon, L., Doval, S., Marcos, A., Bruña, R., & Maestú, F. (2023). Episodic memory dysfunction and hypersynchrony in brain functional networks in cognitively intact subjects and MCI: A study of 379 individuals. *GeroScience*, *45*(1), 477–489.

64. Pernet, C. R., Wilcox, R., & Rousselet, G. A. (2012). Robust correlation analyses: False positive and power validation using a new open source Matlab toolbox. *Frontiers in Psychology*, *3*, 606.

65. Wilcox, R. R. (1994). The percentage bend correlation coefficient. *Psychometrika*, *59*, 601–616.

66. Wang, J., Lu, M., Fan, Y., Wen, X., Zhang, R., Wang, B., Ma, Q., Song, Z., He, Y., Wang, J., & Huang, R. (2016). Exploring brain functional plasticity in world class gymnasts: A network analysis. *Brain Structure & Function*, *221*(7), 3503–3519.

67. Garcia-Penton, L., Perez Fernandez, A., Iturria-Medina, Y., Gillon-Dowens, M., & Carreiras, M. (2014). Anatomical connectivity changes in the bilingual brain. *Neuroimage*, *84*, 495–504.

68. Spitzer, B., & Haegens, S. (2017). Beyond the status quo: A role for beta oscillations in endogenous content (re)activation. *eNeuro*, *4*(4), ENEURO.0170-17.2017.

69. Weiss, S., & Mueller, H. M. (2012). "Too Many betas do not Spoil the Broth": The role of beta brain oscillations in language processing. *Frontiers in Psychology*, *3*, 201.

70. Timofeeva, P., Quinones, I., Geng, S., de Bruin, A., Carreiras, M., & Amoruso, L. (2023). Behavioral and oscillatory signatures of switch costs in highly proficient bilinguals. *Scientific Reports*, *13*(1), 7725.

71. Geng, S., Quinones, I., Gil-Robles, S., Pomposo Gastelu, I. C., Bermudez, G., Timofeeva, P., Molinaro, N., Carreiras, M., & Amoruso, L. (2023). Neural dynamics supporting longitudinal plasticity of action naming across languages: MEG evidence from bilingual brain tumor patients. *Neuropsychologia*, *181*, 108494.

72. Buzsaki, G. (2006). *Rhythms of the brain*. Oxford University Press.

73. Harmony, T. (2013). The functional significance of delta oscillations in cognitive processing. *Frontiers in Integrative Neuroscience*, *7*, 83.

74. Liu, H., Li, W., Zuo, M., Wang, F., Guo, Z., & Schwieter, J. W. (2022). Cross-task adaptation effects of bilingual language control on cognitive control: A dual-brain EEG examination of simultaneous production and comprehension. *Cerebral Cortex*, *32*(15), 3224–3242.

75. Liu, H., Zhang, M., Perez, A., Xie, N., Li, B., & Liu, Q. (2019). Role of language control during interbrain phase synchronization of cross-language communication. *Neuropsychologia*, *131*, 316–324.

76. Raichle, M. E., MacLeod, A. M., Snyder, A. Z., Powers, W. J., Gusnard, D. A., & Shulman, G. L. (2001). A default mode of brain function. *Proceedings of the National Academy of Sciences of the United States of America*, *98*(2), 676–682.

77. Smallwood, J., Bernhardt, B. C., Leech, R., Bzdok, D., Jefferies, E., & Margulies, D. S. (2021). The default mode network in cognition: A topographical perspective. *Nature Reviews Neuroscience*, *22*(8), 503–513.

78. Deco, G., Sanz Perl, Y., de la Fuente, L., Sitt, J. D., Yeo, B. T. T., Tagliazucchi, E., & Kringelbach, M. L. (2023). The arrow of time of brain signals in cognition: Potential intriguing role of parts of the default mode network. *Network Neuroscience*, *7*(3), 966–998.

79. Das, A., de Los Angeles, C., & Menon, V. (2022). Electrophysiological foundations of the human default-mode network revealed by intracranial-EEG recordings during resting-state and cognition. *Neuroimage*, *250*, 118927.

80. Hlinka, J., Alexakis, C., Diukova, A., Liddle, P. F., & Auer, D. P. (2010). Slow EEG pattern predicts reduced intrinsic functional connectivity in the default mode network: An inter-subject analysis. *Neuroimage*, *53*(1), 239–246.

81. Schneider, J. M., Abel, A. D., Momsen, J., Melamed, T. C., & Maguire, M. J. (2021). Neural oscillations reveal differences in the process of word learning among school-aged children from lower socioeconomic status backgrounds. *Neurobiology of Language*, *2*(3), 372–388.

82. Ferre, P., Jarret, J., Brambati, S., Bellec, P., & Joanette, Y. (2020). Functional connectivity of successful picture-naming: Age-specific organization and the effect of engaging in stimulating activities. *Frontiers in Aging Neuroscience*, *12*, 535770.

83. van Dokkum, L. E. H., Moritz Gasser, S., Deverdun, J., Herbet, G., Mura, T., D'Agata, B., Picot, M. C., Menjot de Champfleur, N., Duffau, H., Molino, F., & le Bars, E. (2019). Resting state network plasticity related to picture naming in low-grade glioma patients before and after resection. *Neuroimage Clinical*, *24*, 102010.

84. Lizarazu, M., Carreiras, M., Bourguignon, M., Zarraga, A., & Molinaro, N. (2021). Language proficiency entails tuning cortical activity to second language speech. *Cerebral Cortex*, *31*(8), 3820–3831.

85. Harmelech, T., & Malach, R. (2013). Neurocognitive biases and the patterns of spontaneous correlations in the human cortex. *Trends in Cognitive Sciences*, *17*(12), 606–615.

86. da Silva Castanheira, J., Orozco Perez, H. D., Misic, B., & Baillet, S. (2021). Brief segments of neurophysiological activity enable individual differentiation. *Nature Communications*, *12*(1), 5713.

87. Pliatsikas, C., & Luk, G. (2016). Executive control in bilinguals: A concise review on fMRI studies. *Bilingualism: Language and Cognition*, *19*(4), 699–705.

88. Jeon, H. A., & Friederici, A. D. (2017). What does "being an expert" mean to the brain? Functional specificity and connectivity in expertise. *Cerebral Cortex*, *27*(12), 5603–5615.

89. Jawed, S., Amin, H. U., Malik, A. S., & Faye, I. (2019). Classification of visual and non-visual learners using electroencephalographic alpha and gamma activities. *Frontiers in Behavioral Neuroscience*, *13*, 86.

90. Damoiseaux, J. S., Beckmann, C. F., Arigita, E. J., Barkhof, F., Scheltens, P., Stam, C. J., Smith, S. M., & Rombouts, S. A. (2008). Reduced resting-state brain activity in the "default network" in normal aging. *Cerebral Cortex*, *18*(8), 1856–1864.

91. Humphries, M. D., & Gurney, K. (2008). Network 'Small-World-Ness': A Quantitative Method for Determining Canonical Network Equivalence. *PLoS ONE*, *3*(4), e0002051.